

Computational Physics

Project 4



UiO • University of Oslo

Hunter Wilhelm Phillips (*hunterp*)

November 19, 2018

GitHub Repository at

https://github.com/robolux/Computational_Physics

Abstract

This project explores the application of the Ising model for a 2-dimensional squared lattice. The Metropolis algorithm was implemented to compute the probability rates of transitions during the Monte Carlo simulations being performed. Analytical and numerical results are compared to determine the accuracy of the simulation. The efficiency of the program and Metropolis algorithm are analyzed to ensure large lattice sizes can run. Lars Onsager's analytical solution for the critical heat of a large lattice is also verified numerically with the simulation. It was shown that higher temperatures result in greater instability within the system. This was also coupled with an increasing total energy and decreasing total magnetization for a rise in temperature. The results concluded in the confirmation of a successful algorithm being ran to simulate the Ising model for this particular set of cases.

1. Discussion of Problem Statement

In this project, the goal is to study the Ising model for a $L \times L$ lattice with periodic boundary conditions in 2 dimensions. First, a simple $L = 2$ lattice is to be examined analytically to provide a basis for comparison. Second, the simulation of the Ising model should be programmed and tested with a $L = 2$ lattice. This should be directly compared with the analytical results to determine acceptable convergence. Third, a lattice with $L = 20$ is to be computed with both ordered and random spin orientations. To add another facet into this part of the analysis, it should be run with $T = 1.0$ and $T = 2.4$. This should allow for discussion on the equilibrium time and amount of accepted configurations dependent on T . Fourth, the probability distributions of a lattice with $L = 20$ is to be analyzed with $T = 1.0$ and $T = 2.4$ and the variance computed. Fifth, phase transitions are to be studied numerically using lattices in the set $[40, 60, 80, 100]$ and $T \in [2.0, 2.3]$ with a time step of 0.05. The mean energy $\langle E \rangle$, mean magnetization \mathcal{M} , specific heat C_V , and susceptibility χ are to be computed for visual analysis. Sixth, the critical temperature is to be computed numerically and verified to be within an acceptable error range of the analytical solution. Through this, the tasks at hand have been laid out and the theory and methods explaining the solution are described in *Section 2*.

2. Discussion of Theory & Methods

2.1 The General Ising Model

Assuming that the formation of a d -dimensional lattice is coupled in a set of Λ adjacent lattice positions. For each lattice elemental location, $k \in \Lambda$, there is a representation of the spin of the element \uparrow and \downarrow in the form of a discrete variable $\sigma_k \in \{+1, -1\}$. Each individual spin configuration σ is connected to a specific state of the lattice.

If there are two elemental locations, i and j , in the set, one of them will have an interaction J_{ij} . This same characteristic site will also have an external magnetic field h_j coupled with it. The energy of the system specified can be given by the following Hamiltonian as seen in (1):

$$E = H(\sigma) = - \sum_{\langle ik \rangle} J_{ij} \sigma_i \sigma_j - \mu \sum_j h_j \sigma_j \quad (1)$$

Where the first summation is over pairs of adjacent spins

$\langle ij \rangle$ displays that i and j are nearest neighbors

μ is the magnetic moment

The Boltzmann distribution gives us the probability of a certain configuration as shown in (2):

$$P_\beta(\sigma) = \frac{e^{-\beta H(\sigma)}}{Z_\beta} \quad (2)$$

Where Z_β is the normalization constant

The functioning $\beta = (k_B T)^{-1}$

This showcases that an increase in temperature directly affects the possibility of finding a system in a particular configuration in a negative manner.

This leads into the characterization of a magnetic system and the most important expected values to be calculated. The first is mean energy as seen in (3).

$$\langle E \rangle = \sum_{i=1}^M E_i P_\beta(\sigma) = \frac{1}{Z} \sum_{i=1}^M E_i e^{-\beta E_i} \quad (3)$$

Where M signifies the number of possible configurations

The second is mean magnetization as seen in (4).

$$\langle \mathcal{M} \rangle = \sum_{i=1}^M \mathcal{M}_i P_\beta(\sigma) = \frac{1}{Z} \sum_{i=1}^M \mathcal{M}_i e^{\beta E_i} \quad (4)$$

Where $\mathcal{M}_i = \sum_{j \in \Lambda} \sigma_j$ is represented for all configurations σ

The third is magnetic susceptibility as seen in (5).

$$\chi = \frac{1}{k_B T} (\langle \mathcal{M}^2 \rangle - \langle \mathcal{M} \rangle^2) \quad (5)$$

The fourth is heat capacity as seen in (6).

$$C_V = \frac{1}{k_B T^2} (\langle E^2 \rangle - \langle E \rangle^2) \quad (6)$$

These reduced equations form the basis for the project and allow for the specific model to be deduced. The Ising model can be classified as having a ferromagnetic interaction if $J_{ij} > 0$ and for the purposes of this simulation, this case will be used.

2.2 Simplified Ferromagnetic Ising Model

To ease the complexity of this project, the general Ising model as described in *Section 2.1* will be simplified [1]. The first step is to assume that there is no external magnetic field in play and with this assumption, (1) has its second summation go to zero, leaving (7):

$$E = H(\sigma) = - \sum_{\langle ik \rangle} J_{ij} \sigma_i \sigma_j \quad (7)$$

The coupling constant J is assumed to be a constant which enables the removal of it from within the summation forming (8).

$$E = H(\sigma) = -J \sum_{\langle ik \rangle} \sigma_i \sigma_j \quad (8)$$

The final assumption is that the model is ferromagnetic in nature which means that neighboring spins are aligned, resulting in lower energies.

2.3 Case: $L = 2 \times 2$ Ising Model

To prepare for later comparisons with numerical results, the analytical expressions for an $L = 2 \times 2$ case are explored. Using (3), (4), (5), and (6); the following, Table 1, shows all of possible states for an $L = 2 \times 2$ case.

| State | Symmetries | Energy (J) | Mean Magnetization |
|--|------------|------------|--------------------|
| $\begin{array}{cc} \uparrow & \uparrow \\ \uparrow & \uparrow \end{array}$ | 1 | -8 | 4 |
| $\begin{array}{cc} \uparrow & \uparrow \\ \uparrow & \downarrow \end{array}$ | 4 | 0 | 2 |
| $\begin{array}{cc} \uparrow & \uparrow \\ \downarrow & \downarrow \end{array}$ | 4 | 0 | 0 |
| $\begin{array}{cc} \uparrow & \downarrow \\ \downarrow & \uparrow \end{array}$ | 2 | 8 | 0 |
| $\begin{array}{cc} \downarrow & \downarrow \\ \downarrow & \uparrow \end{array}$ | 4 | 0 | -2 |
| $\begin{array}{cc} \downarrow & \downarrow \\ \downarrow & \downarrow \end{array}$ | 1 | -8 | -4 |

Table 1: Case L = 2 x 2 all 16 Possible Configurations

To compute all the associated physical quantities as shown above, the closed form expressions can be given by the following partition function (9):

$$Z = \sum_{i=1}^1 6e^{-\beta E_i} = e^{\beta 8J} + 12 + 2e^{-\beta 8J} + e^{\beta 8J} = 4 \cosh(8\beta J) + 12 \quad (9)$$

This leads to the expected energy forming into (10):

$$\langle E \rangle = -\frac{\partial}{\partial \beta} \ln Z = -\frac{\partial}{\partial \beta} \ln(4 \cosh(8\beta J) + 12) = -8J \frac{\sinh(8\beta J)}{\cosh(8\beta J) + 3} \quad (10)$$

Using (4) the mean magnetization for this particular system can be computed into (11)

$$\langle \mathcal{M} \rangle = \frac{1}{Z} (-4e^{8\beta J} - 8e^0 + 8e^0 + 8e^{8\beta J}) = 0 \quad (11)$$

This leads to the expected absolute magnetization coming out as (12):

$$\langle \mathcal{M} \rangle = \frac{1}{Z} (-4e^{8\beta J} - 8e^0 + 8e^0 + 8e^{8\beta J}) = \frac{4 + 2e^{8\beta J}}{\cosh(8\beta J) + 3} \quad (12)$$

The expected value for specific heat is characterized in (13):

$$\langle C_V \rangle = \frac{1}{k_b T^2} \frac{\partial^2}{\partial \beta^2} \quad (13)$$

By inserting (10) into (13) the expected specific heat analytical equation (14):

$$\begin{aligned} \langle C_V \rangle &= \frac{1}{k_b T^2} \frac{\partial}{\partial \beta} \left(-8J \frac{\sinh(8\beta J)}{\cosh(8\beta J) + 3} \right) \\ &= \frac{1}{k_b T^2} \left(64J^2 \frac{\cosh(8\beta J)}{\cosh(8\beta J) + 3} - 64J^2 \frac{\sinh^2(8\beta J)}{(\cosh(8\beta J) + 3)^2} \right) \end{aligned} \quad (14)$$

Rewriting (5) into (15) gives the basis for the susceptibility of magnetism:

$$\chi = \frac{1}{k_B T} \sigma_{\mathcal{M}}^2 \quad (15)$$

By combining (11) and (12) into (16), the second integral part for the susceptibility of magnetism can be derived:

$$\sigma_{\mathcal{M}}^2 = \langle \mathcal{M}^2 \rangle - \langle \mathcal{M} \rangle^2 = \frac{32}{Z} (e^{8\beta J} + 1) - 0 = \frac{8 + 8e^{8\beta J}}{\cosh(8\beta J) + 3} \quad (16)$$

Finally, by inserting (16) into (15), (17) can be formulated:

$$\chi = \frac{8 + 8e^{8\beta J}}{k_B T (\cosh(8\beta J) + 3)} \quad (17)$$

These analytical results are the basis for future comparisons with numerically obtained results.

3. Discussion of Algorithms

3.1 Ising Class

To expand on the object orientation programming approach explored in Project 3, the same class structure theory was implemented into this project. All computations and writing to files is completed within the class structure enabling easy future expandability of the coding framework. This allows for seamless calling from unit testing and user interface scripts. The most important

functions held within are *metropolis* and *solve*, with the following sections going into detail further about their functionality.

3.2 Metropolis

The key facet to the successful simulation of the Ising model is a core algorithm that can produce random samples from a probability distribution. The traditional form of direct sampling is beyond difficult to achieve due to the complete partition function being needed to express the probability distribution. The beauty in the Metropolis algorithm is that it only requires a function proportional to the distribution density.

Metropolis Implementation

```
def metropolis(self,w):  
  
    L = int(self.L)  
    for iterable in xrange(L*L):  
        i,j = np.random.randint(1,L+1,2)  
        dE_t = 2.*self.spin_mat[i,j]*(self.spin_mat[i,j+1] + \  
            self.spin_mat[i,j-1] + self.spin_mat[i+1,j] + self.spin_mat[i-1,j])  
        if dE_t <= 0:  
            self.flip(i,j)  
            self.E += dE_t  
            self.M += 2.*self.spin_mat[i,j]  
            self.accepted += 1  
        else:  
            if np.random.random() <= w[8+int(dE_t)]:  
                self.flip(i,j)  
                self.E += dE_t  
                self.M += 2.*self.spin_mat[i,j]  
                self.accepted += 1
```

A proposed move is only implemented with the basis of a transition probability coupled with an acceptance probability. The main advantage of this approach is that the transition probability does not need to be known.

3.3 Monte Carlo

Each Cycle of the Monte Carlo simulation is fairly straightforward and essentially is a framework for obtaining mass amount of data points from *metropolis*. A simple snippet from

solve can be seen below, showing a Monte Carlo simulation loop, which calls metropolis for each Monte Carlo cycle to be performed until the maximum number of cycles is reached.

Monte Carlo Implementation

```
while cycle < MCC:  
    self.metropolis(w)  
    avg[0] += self.E; avg[1] += self.E**2  
    avg[2] += self.M; avg[3] += self.M**2  
    avg[4] += abs(self.M)  
    cycle += 1  
self.average(avg,T,cycle,filename)
```

3.4 Parallelization

When running larger test cases with lattice sizes reaching up to 100×100 it was recommended that we use a pool based multiprocessing framework to parallelize the code. This would enable each thread on the CPU to solve a specific case. At first this seemed fairly trivial, although it ended up being incredibly frustrating and complex. Since this was a pure Python implementation, *mpi4py* (uses the *MPI* C library) and *multiprocessing* were analyzed for use. The main drawback of *mpi4py* is that its documentation is not as good as pure *MPI*, leaving a lot of questions unanswered. This led to *multiprocessing*; with the specific function, *pool*, being explored further.

All was going well until both libraries produced a *PicklingError* upon execution. Upon further research into the documentation it appears that bound methods cannot be pickled. In *mpi4py* the underlying *MPI* C library uses cpickle while *multiprocessing* uses pickle, both failing to properly pickle the methods for parallelization. This would require a complete program rewrite and defeat the purpose of the beautiful object orientation currently in use.

Since this was not feasible to implement in a reasonable amount of time, the runs were just performed in a successive order, which worked fine for obtaining the results. However, the issue was explored deeper for future projects. It appears that there is a fork of *multiprocessing* called *pathos.multiprocessing* that uses dill to serialize almost everything, including bound methods [2]. It appears that this library would work and be able to create appropriate parallel pools with the dill pickled methods.

4. Discussion of Results

4.1 System Specifications

A few notes about the system running the algorithms before analyzing the results should be helpful in determining performance between different computers as seen in *Table 2*.

| | |
|------------------|--------------------|
| Operating System | Mac OS X |
| Processor | i7 - 2.2 GHz |
| Memory | 8 GB 1600 MHz DDR3 |
| Hard drive | 128 GB SSD |

Table 2: System Specifications

With the conditions under test being established we can now dive into the data recorded.

4.2 Ising Model with $L = 2 \times 2$

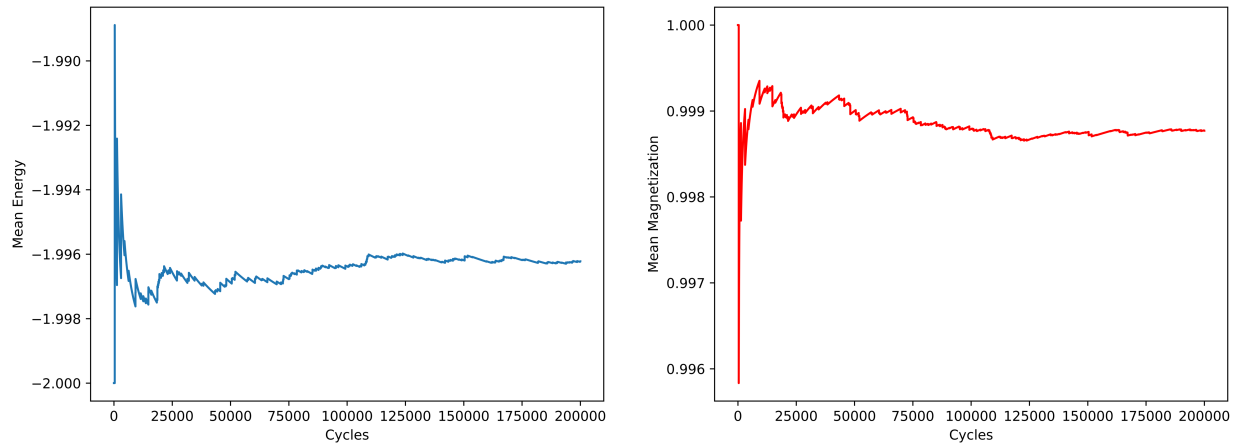
The first test of the project was to use a simple 2×2 lattice with a $T = 1.0$ across a range of Monte Carlo cycles in the set of $[1e3, 1e4, 1e5, 1e6]$. The mean energy $\langle E \rangle$, mean magnetization \mathcal{M} , specific heat C_V , and susceptibility χ were calculated to provide units of comparison. These numerical results were then compared with the analytical solution as showcased below in *Table 3*.

| M | $\langle E \rangle$ | C_V | χ | \mathcal{M} |
|------------|---------------------|----------|----------|---------------|
| 1e3 | -1.99600 | 0.031936 | 0.001996 | 0.99900 |
| 1e4 | -1.99580 | 0.033529 | 0.005090 | 0.99845 |
| 1e5 | -1.99604 | 0.031617 | 0.004133 | 0.99865 |
| 1e6 | -1.99595 | 0.032318 | 0.004039 | 0.99865 |
| Analytical | -1.99598 | 0.03208 | 0.004010 | 0.99865 |

Table 3: Comparison between Monte Carlo simulations at different length and the analytical solution for a $L = 2 \times 2$ system

It appears that a lot of Monte Carlo cycles does improve the solution but only to a small extent. For the sake of choosing a number that achieves a good agreement, it appears that 1e5 cycles is a stable and solid choice. To verify this decision and provide a buffer zone for convergence, a test was run with 2e5 cycles as seen below in Figure 1.

Figure 1: Random Spin Orientation of $L = 2 \times 2$ over 2e5 cycles with $T = 1.0$
Mean Energy (left) and Mean Magnetization (right)



It can be seen that the solution stabilizes nicely, validating the decision to provide a doubling multiplier of convergence space, resulting in 2e5 being the optimal amount of Monte Carlo cycles for this particular case

4.3 Ising Model with $L = 20 \times 20$

With the verification that the model works on a lattice size of 2×2 , it was time to expand it into a lattice size of 20×20 . It can be assumed that all *Figures* in *Section 4.3* are with a lattice size of 20×20 . The first task was to compute and plot *Figures 2 – 5* for analysis.

**Figure 2: Mean Energy with $T = 1.0$ and $1e4$ Monte Carlo Cycles
Ordered (Left) and Random (Right)**

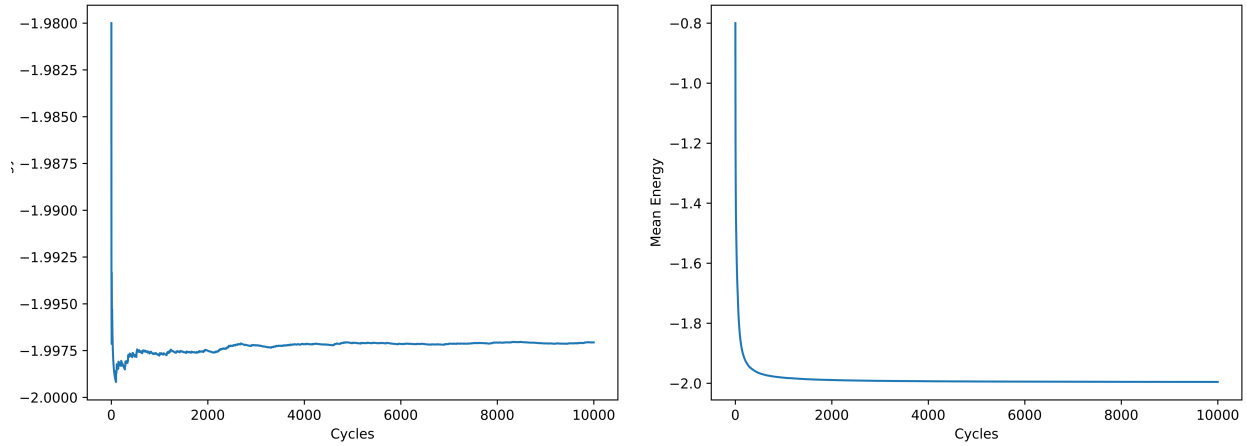


**Figure 3: Mean Energy with $T = 2.4$ and $1e4$ Monte Carlo Cycles
Ordered (Left) and Random (Right)**

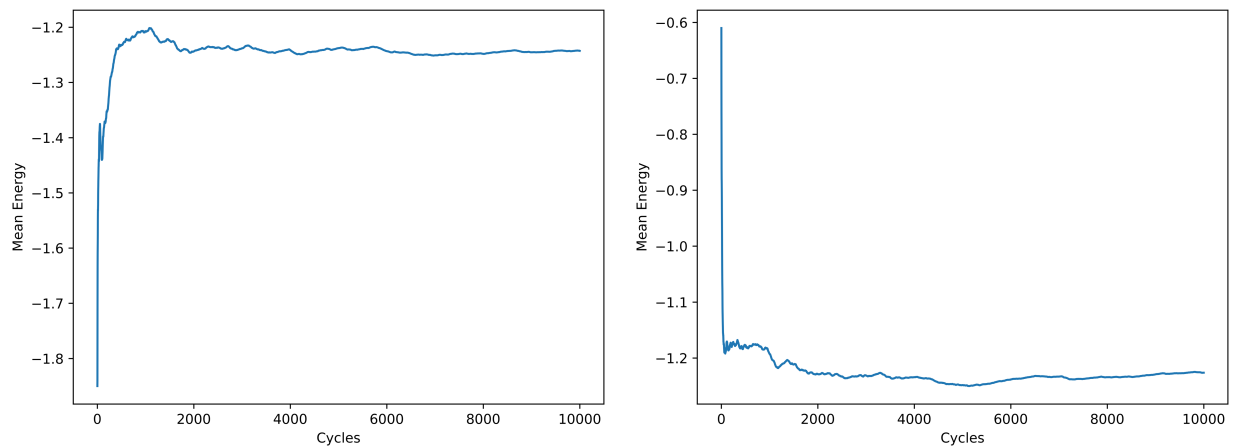


**Figure 4: Mean Magnetization with $T = 1.0$ and $1e4$ Monte Carlo Cycles
Ordered (Left) and Random (Right)**

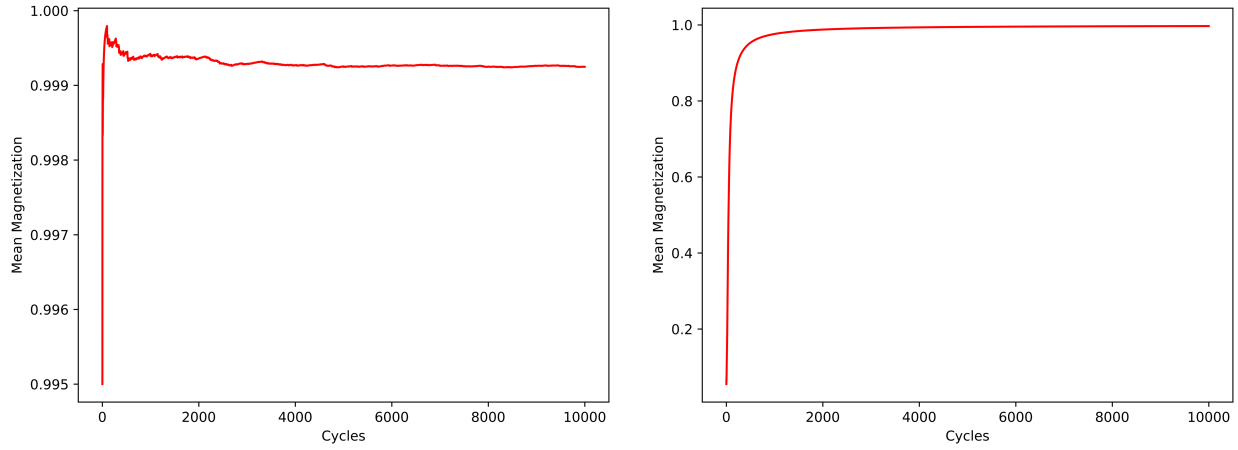
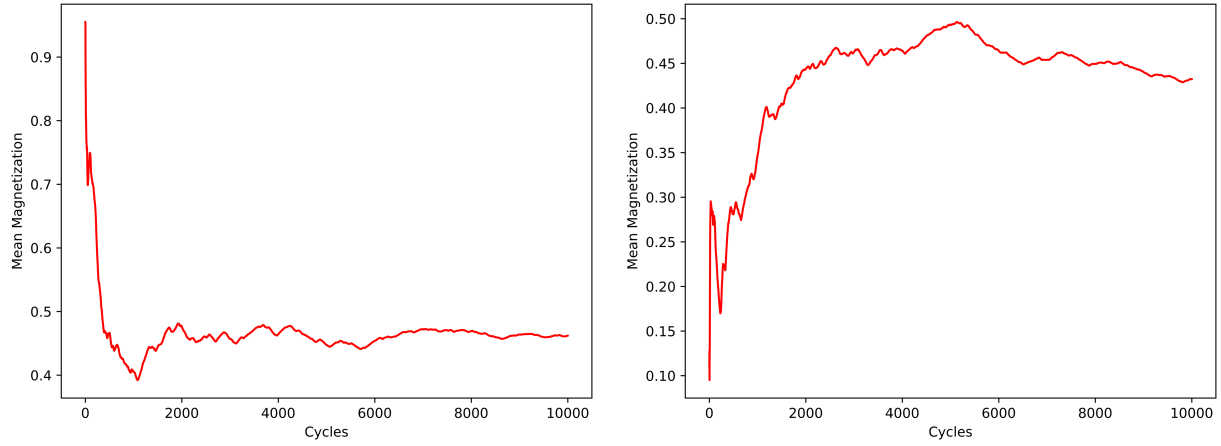


**Figure 5: Mean Magnetization with $T = 2.4$ and $1e4$ Monte Carlo Cycles
Ordered (Left) and Random (Right)**



The first comparison is between the random and ordered spin orientations with respect to mean energy. With a $T = 1.0$ as seen in *Figure 2*, it can be seen that the random spin orientation produced a smoother gradient slope towards the desired solution when compared to the ordered spin orientation. With a $T = 2.4$ as shown in *Figure 3*, both spin orientations appear to converge to the solution, but with greater noise. This can be attributed to the fact that the higher temperature (T) retains a slightly more unstable environment.

The second comparison is between the random and ordered spin orientations with respect to mean magnetization. The same effect can be seen in Figure 4 that was seen in *Figure 2* with a $T = 1.0$. The solution is stable in both and the random configuration initialized case converges quite smoothly. With a $T = 2.4$ the solution has a harder time maintaining stability, although manages to converge within reason as seen in *Figure 5*.

To reach an equilibrium situation for these cases, it would appear that for a 20×20 lattice with a $T = 1.0$, that 2000 Monte Carlo cycles would be appropriate. For a 20×20 lattice with a $T = 2.4$, that 4000 Monte Carlo cycles would be an acceptable stability. It is interesting to note that the temperature roughly doubles and the resulting amount of Monte Carlo cycles needed follows suit. This is the expected outcome and to verify the accepted configuration states, *Figures 6 & 7* were plotted for visual analysis.

**Figure 6: Accepted Configurations with $T = 1.0$ and $1e4$ Monte Carlo Cycles
Ordered (Left) and Random (Right)**

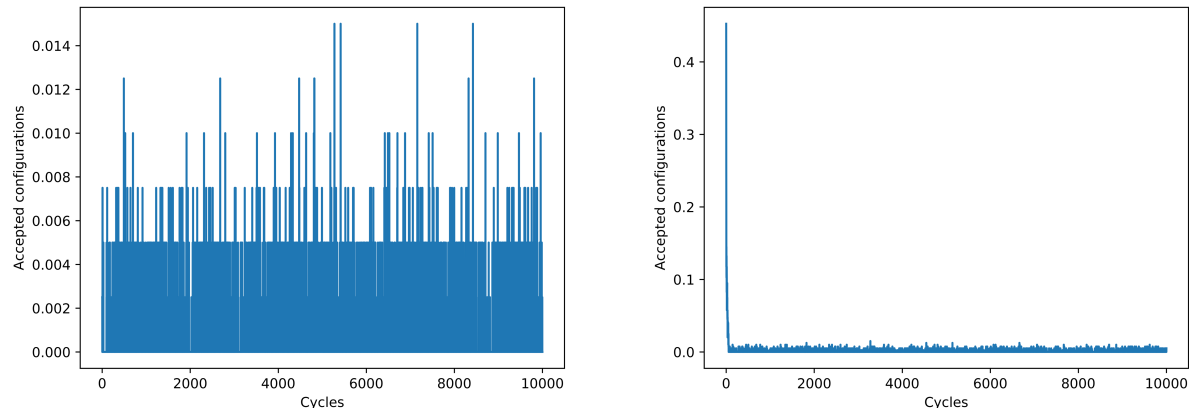
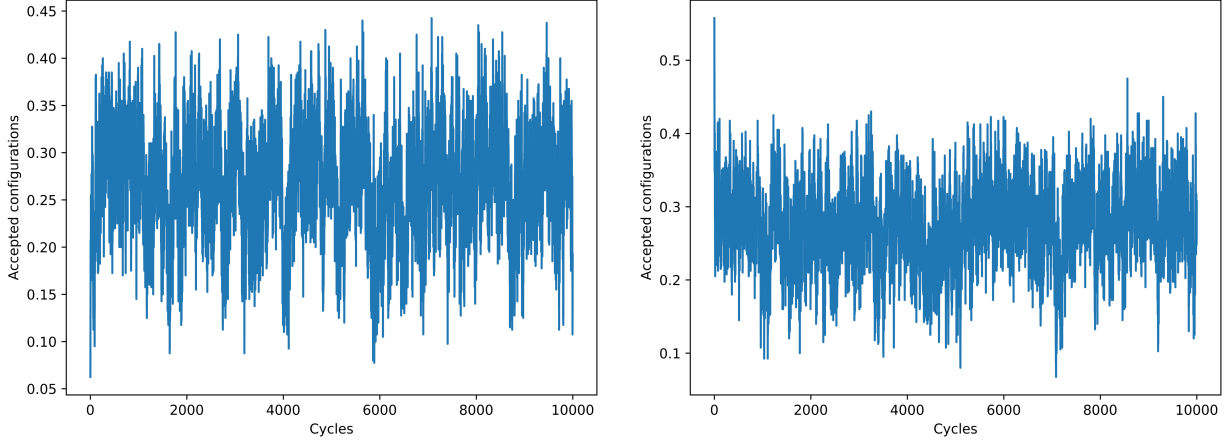


**Figure 7: Accepted Configurations with $T = 2.4$ and $1e4$ Monte Carlo Cycles
Ordered (Left) and Random (Right)**



When the equilibrium state has been reached, the expected rate of accepted configurations should decline. This is elegantly displayed in *Figure 6*, as the small number of accepted configurations for a $T = 1.0$ is predicted with a more stable lower temperature. When this temperature is raised to $T = 2.4$, the amount of accepted configuration drastically increases as shown in *Figure 7*. This is indicative of the large amount of chaos with respect to higher temperatures and the model currently being studied in the simulation.

4.4 Analyzing Probability Distribution

To look at the behavior of the $L = 20 \times 20$ system, *Figures 8 & 9* were produced to analyze the probability distributions.

Figure 8: Probability Distribution of Energy, $T = 1.0$, Ordered (Left) and Random (Right)

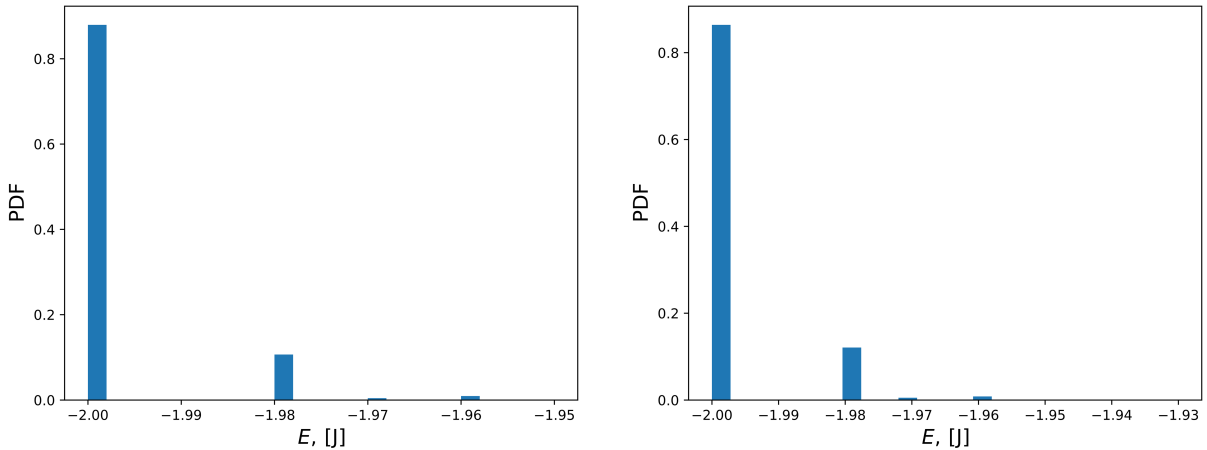
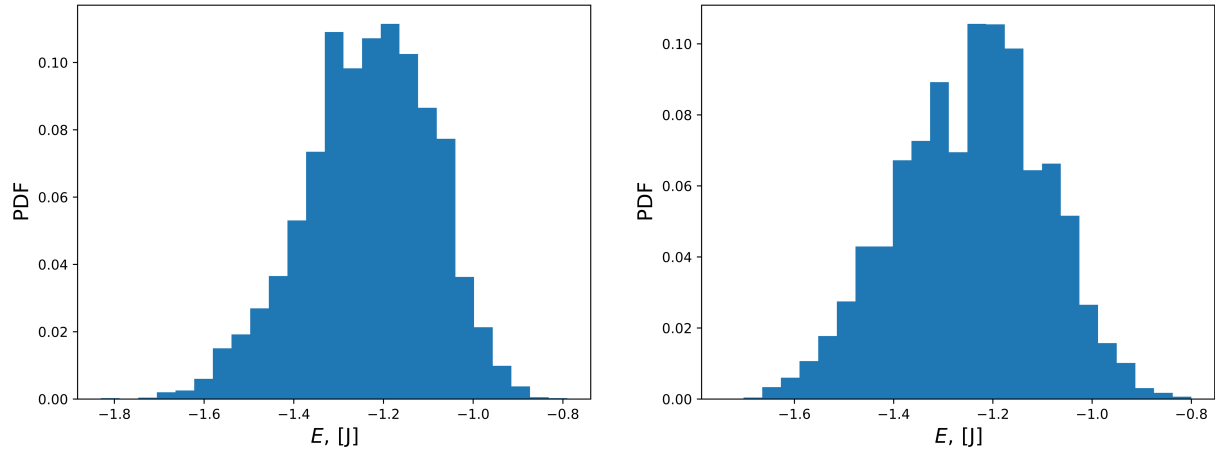


Figure 9: Probability Distribution of Energy, T = 2.4, Ordered (Left) and Random (Right)



It can be seen that the distribution of the energy states with $T = 1.0$ in *Figure 8* produce a right positive skew distribution in both ordered and random spin orientations. The distribution of energy states with $T = 2.4$ in *Figure 9* produces a normal distribution in both ordered and random spin orientations. To further analyze these results, the variance is calculated as shown in *Table 4*.

| | Variance |
|------------------|----------|
| Ordered, T = 1.0 | 0.00781 |
| Random, T = 1.0 | 0.02611 |
| Ordered, T = 2.4 | 0.14240 |
| Random, T = 2.4 | 0.14346 |

Table 4: Calculated Variance for Probability Distributions

The calculated variance for $T = 1.0$ is much tighter due to the nature of the curve, but this is expected with the volatility of higher temperatures in this simulation such as $T = 2.4$ in this case. Upon inspection of *Figures 8 & 9* these values obtained are well within reason as being valid. It is worth noting that these values show the possibility of allowing a curve to be fit to the distribution for a varying computational mean energy.

4.5 Numerical Analysis of Phase Transitions

The algorithm developed was applied to larger lattice sizes of 40, 60, 80, and 100 in order to get the model as realistic as possible. For each lattice case the mean energy $\langle E \rangle$, mean magnetization \mathcal{M} , specific heat C_V , and susceptibility χ were plotted for visual analysis. The temperature range was set to be in the set [2.0, 2.3] with incremental steps of 0.05. These conditions resulted in *Figures 10 – 13* being generated.

Figure 10: Mean Magnetization vs Temperature with a range of Lattice Sizes

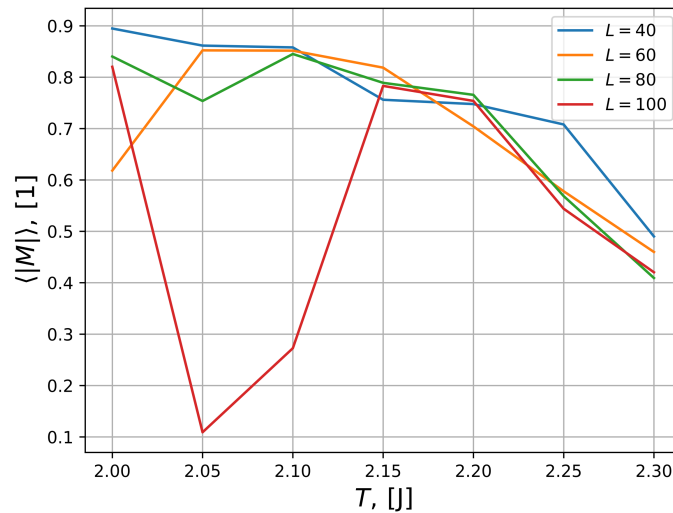


Figure 11: Mean Energy vs Temperature with a range of Lattice Sizes

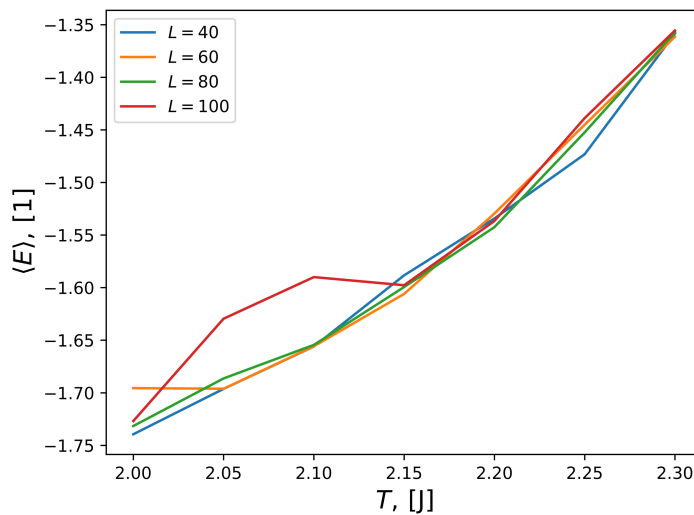


Figure 12: C_v vs Temperature with a range of Lattice Sizes

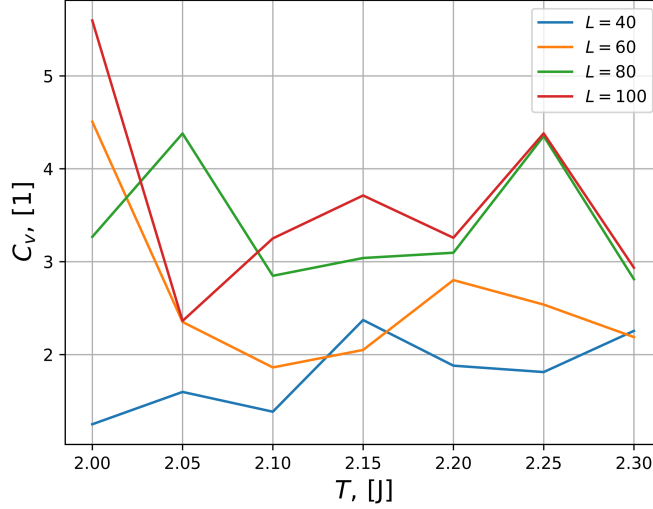
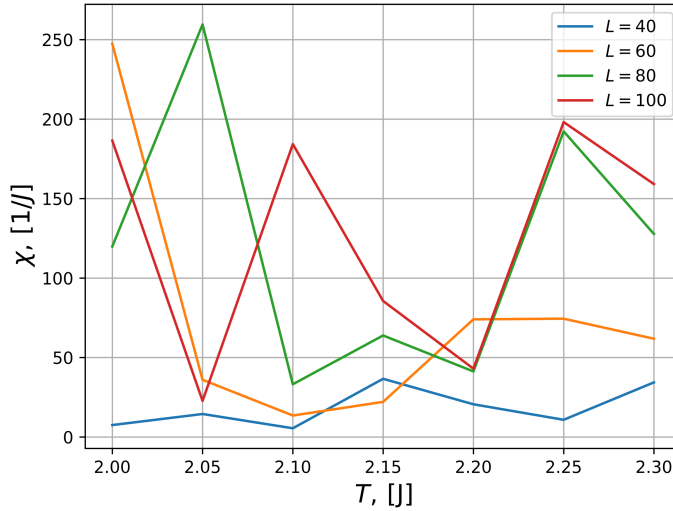


Figure 13: χ vs Temperature with a range of Lattice Sizes



In *Figure 10* the reducing mean magnetization is shown reducing with respect to an increasing temperature, which is the expected result. The energy is expected to rise with an increase in temperature and that is validated in *Figure 11*. There is a possible phase transition being seen in *Figure 10* with the lattice size of 100 x 100, which that same point lying on the x-axis (2.05) being indicated upon in *Figures 11-13*. To further refine these results a smaller temperature increment would be more optimal although the computational time drastically increases with these additional computations. The simulation for example already takes approximately 90 minutes to calculate a $L = 100 \times 100$ matrix with a step size of $T = 0.05$. By reducing the temperature step size this would quickly balloon out of control.

4.6 Critical Temperature Validation

According to [3] the critical temperature is as described below in (18):

$$\frac{kT_c}{J} = \frac{2}{\ln(1 + \sqrt{2})} \approx 2.269 \text{ with } v = 1 \quad (18)$$

Using:

$$T_c(L) - T_c(L = \infty) = aL^{-\frac{1}{v}} \quad (19)$$

Inserting L_i and L_j into (19) and subtracting, (20) can be obtained:

$$\begin{aligned} T_c(L_i) - T_c(L_j) &= a \left(L_i^{-\frac{1}{v}} - L_j^{-\frac{1}{v}} \right) \\ a &= \frac{T_c(L_i) - T_c(L_j)}{L_i^{-\frac{1}{v}} - L_j^{-\frac{1}{v}}} \end{aligned} \quad (20)$$

By selecting the global maximum for each L as described in the lattice set $L = [40, 60, 80, 100]$ it was computed that $a = 0.63$. Rearranging (19) concludes in the calculation of T_c as seen below in (21):

$$\begin{aligned} T_{c_\infty}(L) &= T_c(L) - \frac{a}{L} \\ &= 2.252 \end{aligned} \quad (21)$$

When comparing the values obtained in (18) and (21) it can be seen that they are within the error bound of 0.01 and this is an acceptable result. It is assumed that with a smaller temperature step size, this could be refined, but at the cost of a massive computational time.

5. Conclusion

Through this project, a successful Monte Carlo simulation of the Ising model was created with the implementation of the Metropolis algorithm. The system proved to be reliable for a spin lattice experiencing a second order phase transition, gaining accuracy as the size of the lattice grew. By starting simple with a $L = 2 \times 2$ lattice, the simulation was verified against analytical results with acceptable precision. Upon verification, $L = 20 \times 20$ lattices were computed with a myriad of parameters to observe the Ising model. This showed the increasing accuracy with size, and it was stepped up to larger sizes including a 100×100 lattice. These larger data sets were used to verify numerically the analytical critical temperature to within an error of approximately 0.01. This project concludes in a comprehensive understanding of the Ising model and how to use the Monte Carlo method coupled with the Metropolis algorithm to simulate it effectively.

6. Future Work and Thoughts

I was really excited to work on this project and it was actually the reason I decided to take the course. In robotics, Monte Carlo algorithms are used extensively in robotics with the shining example being Monte Carlo Localization (MCL) [4]. I have been in multiple jobs where senior engineers are implementing MCL into complicated robotics systems and I never had a chance to work with them. It is something rarely discussed in traditional computer science / engineering undergraduate curriculum. This is why I made the transition to taking this course in the Physics department and this project validated that decision entirely. I feel it has given me a firm foundation in the concepts and might give me an edge for positions requiring localization of robots.

The abstract side of my creativity wonders if you could apply the framework of mean energy and mean magnetization to a weighting system in 2D. A typical MCL algorithm uses those positions in space to weigh out localization paths. If you took that and defined permeability zones to cross over phase transitions, you could define multiple movement states of the robot. This means you could change the movement selection based on the environmental conditions, just based on the Monte Carlo simulation with prescribed phase transitions reacting to external states

automatically. Theoretically you could reduce your computational overhead by a factor of the phase locations on your curve.

I honestly feel that this project is just the right amount of work for students to complete. Personally, I think it would be interesting to try anti-ferromagnetic and non-interacting states in the Ising model; if you feel there is ever a need to add some more facets.

7. References

- [1] Hjorth-Jensen, Morten. "Project 4." *Computational Physics FYS3150*, Fall 2018. University of Oslo. Lectures.
- [2] McKerns, Mike. "Pathos." GitHub, GitHub Inc, 25 July 2018, github.com/uqfoundation/pathos.
- [3] Onsager, L., Crystal statistics. I. A two-dimensional model with an order-disorder transition, *Physical Review, Series II*, 65 (3-4), pp. 117-149 (1944).
- [4] Thrun, Sebastian, et al. "Robust Monte Carlo localization for mobile robots." *Artificial intelligence* 128.1-2 (2001): 99-141.